

## Highly Efficient Adenoviral Transduction of Pancreatic Islets using a Microfluidic

### Device

Pamuditha N. Silva<sup>1</sup>, Zaid Atto<sup>1</sup>, Romario Regeenes<sup>1</sup>, Uilki Tufa<sup>1</sup>, Yih Yang Chen<sup>1</sup>, Warren C.W. Chan<sup>1</sup>, Allen Volchuk<sup>3</sup>, Dawn M. Kilkenny<sup>1</sup>, Jonathan V. Rocheleau<sup>1,2,4</sup>

<sup>1</sup>*Institute of Biomaterials and Biomedical Engineering, University of Toronto, CANADA;*

<sup>2</sup>*Department of Physiology, University of Toronto, CANADA;*

<sup>3</sup>*Keenan Research Center of the Li Ka Shing Knowledge Institute, St. Michael's Hospital, CANADA;*

<sup>4</sup>*Toronto General Research Institute, University Health Network, CANADA;*

## Supplemental Experimental

### Nanoparticle Fabrication

Five nm gold nanoparticles (NPs) were synthesized by adding 1 mL of HAuCl<sub>4</sub> (1% w/v) to 80 mL of ultrapure water, and heating to 60°C for 50 min in a 250 mL Erlenmeyer flask. A mixture of 6 mL of sodium citrate tribasic (1% w/v), 1.5 mL tannic acid (1% w/v), 1.5 mL of potassium carbonate (25 mM), and 24 mL of ultrapure water was heated separately to 60°C for 50 min. This mixture was quickly added under vigorous stirring to the Erlenmeyer flask and heated at 60°C for another 30 min. The solution was further heated to 100°C for 10 min, and allowed to cool to room temperature. Subsequently, 1 mL of Bis(p-sulfonatophenyl)phenylphosphine dihydrate dipotassium salt (BSPP; 80 mg/mL) was added to the NP solution and allowed to stir overnight. NPs were subsequently washed with 0.01% v/v Tween20 (Bioshop) via ultracentrifugation at 150,000 g.

Fifteen and 100 nm gold NPs were synthesized using the citrate reduction method. Briefly, 1 mL of 3% w/v sodium citrate tribasic was added to 100 mL of ultrapure water and heated to boil in a 250 mL Erlenmeyer flask. Under vigorous stirring conditions, 1 mL of 1% w/v HAuCl<sub>4</sub> was quickly added to the mixture, and allowed to stir for 10 min after the solution turned cherry red in colour. The flask was placed on ice for 10 min to cool, and left to warm to room temperature for 15 min. This produced 15 nm NPs, which were used as seeds to produce 100 nm NPs. Briefly, 997 µL of 1% w/v HAuCl<sub>4</sub> and 997 µL of 4.4 mg/mL sodium citrate tribasic was added to 96.7 mL of water. To this mixture, 305 µL of the 15 nm NP solution (2.4 nM), was added. Under vigorous stirring conditions, 997 µL of 2.8mg/mL hydroquinone was added to the flask, and allowed to stir overnight for the seeds to nucleate into 100 nm NP.

Prior to surface functionalization, 100 nm NPs were first washed twice with 0.05% w/v sodium citrate tribasic with 0.05% w/v Tween20 in water, and then once in 0.05% w/v sodium citrate tribasic. Fifteen nm NPs were ready to be surface functionalized directly after citrate reduction synthesis. Both types of NPs were surface functionalized with a polyethylene glycol (PEG) mixture that consisted of 85% SH-PEG(5kDa)-CH<sub>3</sub> and 15% SH-PEG(5kDa)-NH<sub>2</sub> (both

from Laysan Bio.). Briefly, the NPs were incubated at 60°C for 1 hour with the PEG mixture at a concentration of 10 PEG molecules per square nanometer of particle surface area, diluted from a stock 1 mg/mL solution of the PEG mixture. NPs were subsequently washed twice with a solution of 0.05% w/v sodium citrate tribasic with 0.05% w/v Tween20, and then washed once with just 0.05% w/v sodium citrate tribasic. All washing steps are done via centrifugation (150,000 g for 5 nm NPs, 15,000 g for 15 nm NPs, and 600 g for 100 nm NPs.) All spin cycles lasted 35 min.

NPs were fluorescently tagged by reacting Cyto633-NHS (CytoDiagnostics) with the free amine groups on the NP surface. Fluorophore was incubated in 10 molar excess with the nanoparticles overnight at 4°C, and subsequently washed as described previously (1-3).

### **Particle Image Velocimetry (PIV) and Particle Tracking**

Freshly isolated islets were loaded into devices with one of the three islet holding area designs (i.e., “Spiral 1”, “Spiral 2” or “Spiral 3”). Islets were loaded into the devices as described previously. Cy5 labelled nanoparticles with a core diameter of 100 nm and diluted to  $2.9 \times 10^{-4}$  nM were flowed at 100  $\mu$ L/hr. Hydrodynamic traps of the device were imaged with a 20 $\times$ /0.8 NA air objective of a scanning LSM710 confocal microscope (Carl Zeiss) with 633 nm wavelength laser line. The field of view was rotated in such a way that all hydrodynamic traps shared the same alignment during image acquisition. Each time series was 50 frames at a frame-rate of 1 every 0.97 seconds. An Otsu threshold was applied to the nanoparticle channel, creating a processed time series. Cross-correlation analysis of sequential images was performed on ImageJ with open source plugins (4) and averaged on Matlab 2009a. Magnitude plots were analyzed on ImageJ. Cumulative particle counts within a region of interest defined as a 30- $\mu$ m tall band above islets were measured using an object counter plugin with the processed time series.

### **References**

1. Ghosh K, Kanapathipillai M, Korin N, McCarthy JR, & Ingber DE (2011) Polymeric nanomaterials for islet targeting and immunotherapeutic delivery. *Nano letters* 12(1):203-208.
2. Chou LY, Zagorovsky K, & Chan WC (2014) DNA assembly of nanoparticle superstructures for controlled biological delivery and elimination. *Nature nanotechnology* 9(2):148-155.
3. Paciotti GF, et al. (2004) Colloidal gold: a novel nanoparticle vector for tumor directed drug delivery. *Drug delivery* 11(3):169-183.
4. Tseng Q, et al. (2011) A new micropatterning method of soft substrates reveals that different tumorigenic signals can promote or reduce cell contraction levels. *Lab on a chip* 11(13):2231-2240.

## Supplemental Figure Legends

**Figure S1: Design and *in silico* simulation of a microfluidic device featuring eight hydrodynamic traps arranged in parallel.** (A) Schematic representation of three islet holding area designs. The initial design, Spiral 1, featured 8 hydrodynamic traps connected in parallel with a fixed width main channel (widths at various positions indicated by double-headed arrows). In Spiral 2, the width of the main channel from the exit of each hydrodynamic trap was increased according to the modelled pressure drop across uniform islets. The final design, Spiral 3, was a second iteration featuring further increases in main channel width. (B) Schematic representation of three scenarios of islets (*yellow*) loaded in the hydrodynamic traps. Islets with uniform geometry (*green* channel) were modelled as 200  $\mu\text{m}$  diameter ellipsoids while non-uniform islets (*red* channel) had varying geometries. Incomplete loading featured the same non-uniform islet content as the red channel with the exception that the third hydrodynamic trap was empty (*blue* channel). (C) Fluid flow around islets of varying geometries and configurations was modelled on COMSOL Multiphysics and variability in pressure drop ( $\Delta P$ ) was measured relative to the value across the islet in the first hydrodynamic trap (as indicated). All three simulations revealed a high degree of  $\Delta P$  variability for Spiral 1, but improved with the Spiral 2 design. Islets modelled in Spiral 3 featured the lowest  $\Delta P$  variability in all three simulations. The islet holding area of Spiral 3 was implemented in the final design of the microfluidic device used in these studies.

**Figure S2: Particle tracking and Particle Image Velocimetry (PIV) validate Spiral 3 design performance.** (A) Representative image of fluorescent nanoparticles (in red) overlaid onto a DIC image of islets loaded into a hydrodynamic trap. A 30  $\mu\text{m}$  tall band (in *yellow*) above the islet defines the region of interest (ROI) where particle counts were collected. Scale bar represents 50  $\mu\text{m}$ . (B) Average cumulative count of particles that passed through the ROI in (A) during a 50-frame time series for Traps 1, 4 and 7 shows a progressively decreasing variability from Spiral 1, 2 and 3. N=4 separate experimental runs with 7-8 islets loaded in each device. (C) Representative heat map of particle speeds around islet resting in hydrodynamic trap of Spiral 3 (DIC image overlay). (D) Box and whisker plot of average speed in all hydrodynamic traps. Spiral 3 exhibits the least fluid speed variability between traps, predicting a relatively even viral load to all islets loaded in device. N=6 separate experimental runs with 7-8 islets loaded in each device.

**Figure S3: Short-term treatment with EDTA treatment expands islet intercellular space.** (A) Representative confocal image slices acquired 24  $\mu\text{m}$  from the base of an islet surrounded by fluorescent dextran. Image sequence reveal flow of fluorescent dextran around and within a representative islet treated with increasing concentrations of

EDTA (*as indicated*). **(B)** Extended focus projection of each image series along the z-axis reveals an extensive and tortuous intercellular space that expands in islets exposed to increasing concentrations of EDTA. Scale bars represent 50  $\mu\text{m}$ . **(C)** The integrated surface area to volume ratio reveals that 2 mM EDTA is sufficient to produce the greatest increase in intercellular space. N = 4 - 5 islets for each EDTA concentration.

**Figure S4:  $\text{Ca}^{2+}$  chelation increases media exchange rate.** **(A)** A time-series of fluorescent dextran (70 kDa) flown into an islet-loaded trap at 300  $\mu\text{L/hr}$  in the absence of (-) EDTA. Media initially exiting the islet produces a clear (non-fluorescent) tail that disappears faster in islets treated with (+) EDTA **(B)**. Scale bar represents 50  $\mu\text{m}$ . **(C)** Plotting the time between fluorescent dextran appearance and disappearance of the clear tail against varying flow rates reveals a consistent increase in media exchange rate in the presence (*green*) compared to the absence (*red*) of EDTA.

**Figure S5: EDTA-treated islets after 24 hours of recover show glucose-stimulated  $\text{Ca}^{2+}$ -influx characteristic of first phase insulin secretion.** **(A)** Three representative image series of fluo-4 stained islets during glucose stimulation (2 mM to 10 mM). Islets were imaged 24 hours after a 75-minute exposure to 2 mM EDTA and 200  $\mu\text{L/hr}$  flow in the microfluidic device. Scale bars in images represent 20  $\mu\text{m}$ . **(B)** Fluorescence intensity traces during glucose stimulation. Horizontal scale bar represents 2 min and vertical scale bar represents 1-fold normalized intensity.

**Movie S1: Single islets load into device sequentially.** Time series of four murine islets being loaded sequentially into hydrodynamic traps during gravity-driven flow. Scale bar indicates 300  $\mu\text{m}$ .

**Movie S1: EDTA-induced islet expansion is reversible.** Confocal time series of fluorescent dextran (*red*) and 100 nm nanoparticles (NPs; *green*) flowing through an islet superimposed on the white light image. Part 1 of the movie demonstrates the effect of flowing 2 mM EDTA at 200  $\mu\text{L/hr}$  for 30 minutes. As the cell-cell adhesions begin to dissociate, dextran fills the intercellular space. The islet continued to expand for an additional 45 minutes (not shown) before the next time series (shown in Part 2) was collected. In Part 2, fresh media (*i.e.*, 0 mM EDTA) without NPs was flown through the device for 30 min at 200  $\mu\text{L/hr}$ . In the absence of EDTA, and therefore in the presence of free  $\text{Ca}^{2+}$ , the cells begin to contract and the intercellular space slowly shrinks. A few NPs appear to become trapped in the contracting intercellular space. Scale bar represents 50  $\mu\text{m}$ .

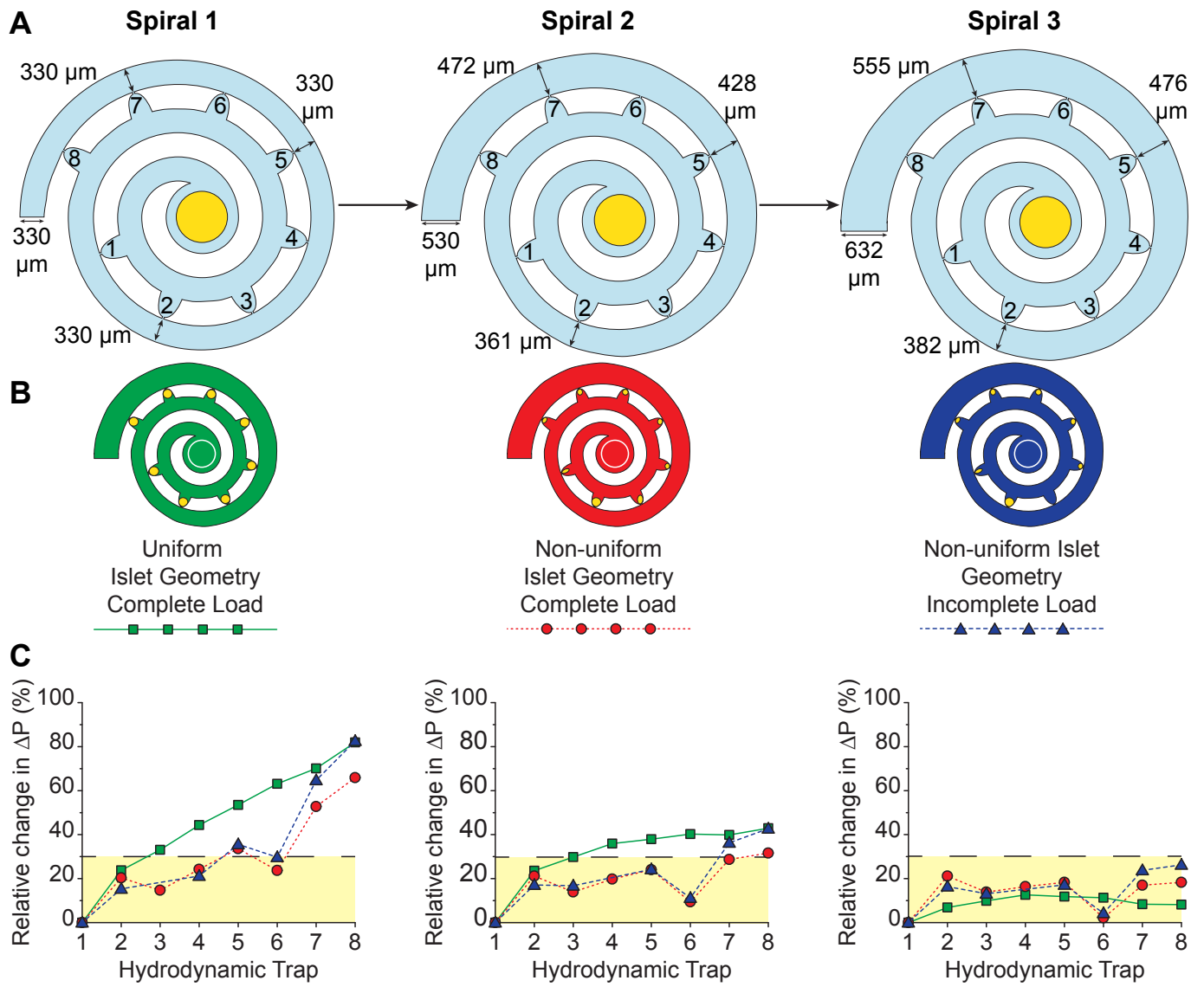


Figure S1

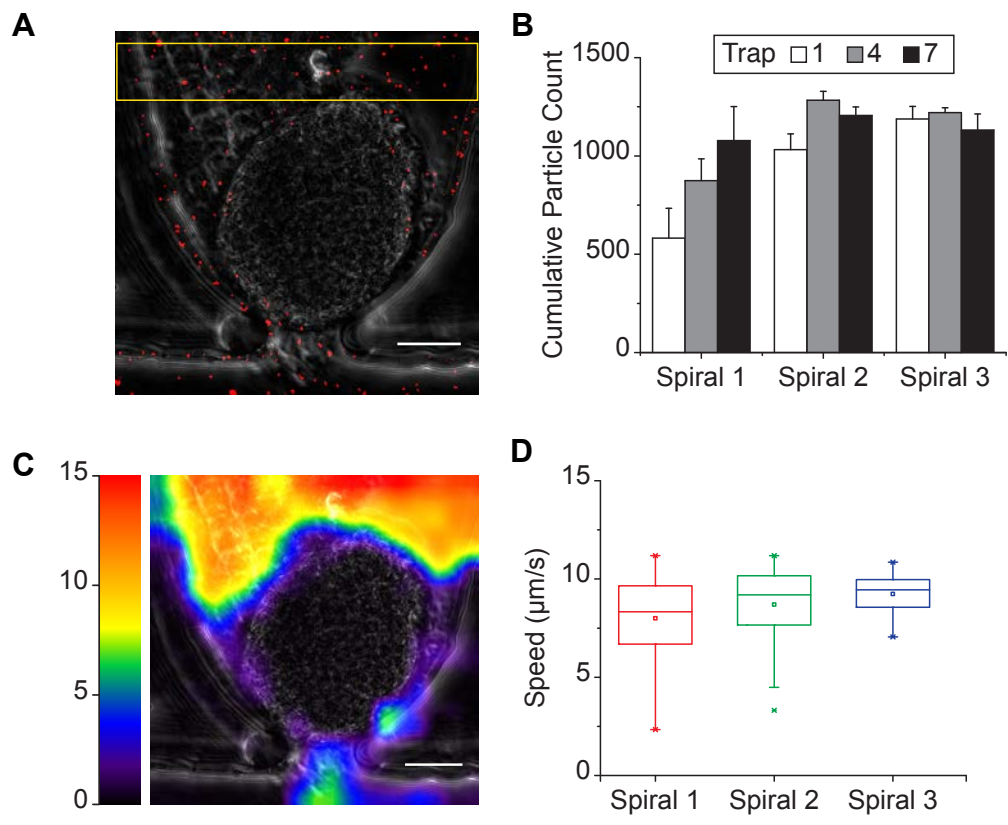


Figure S2

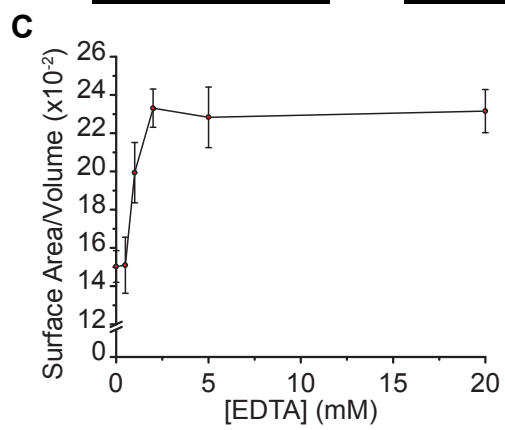
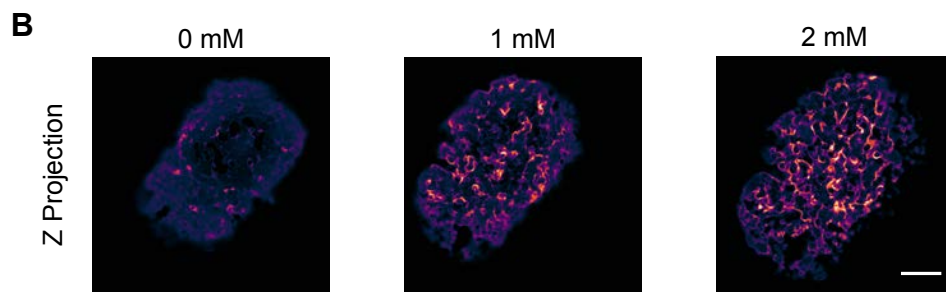
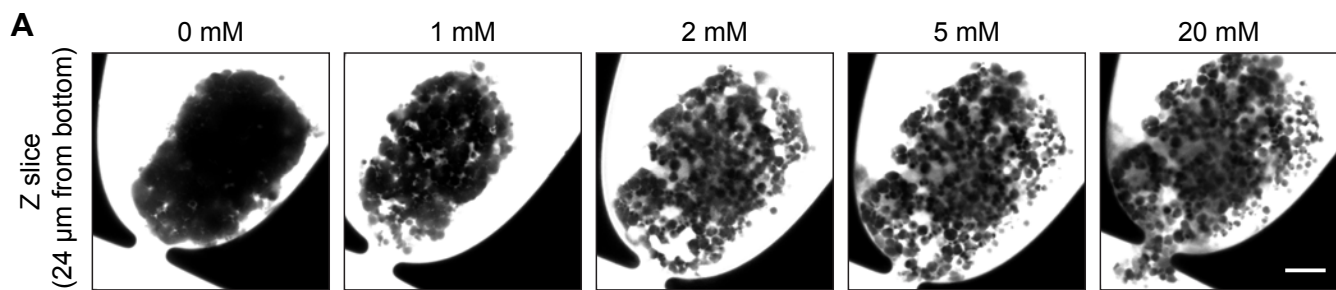


Figure S3

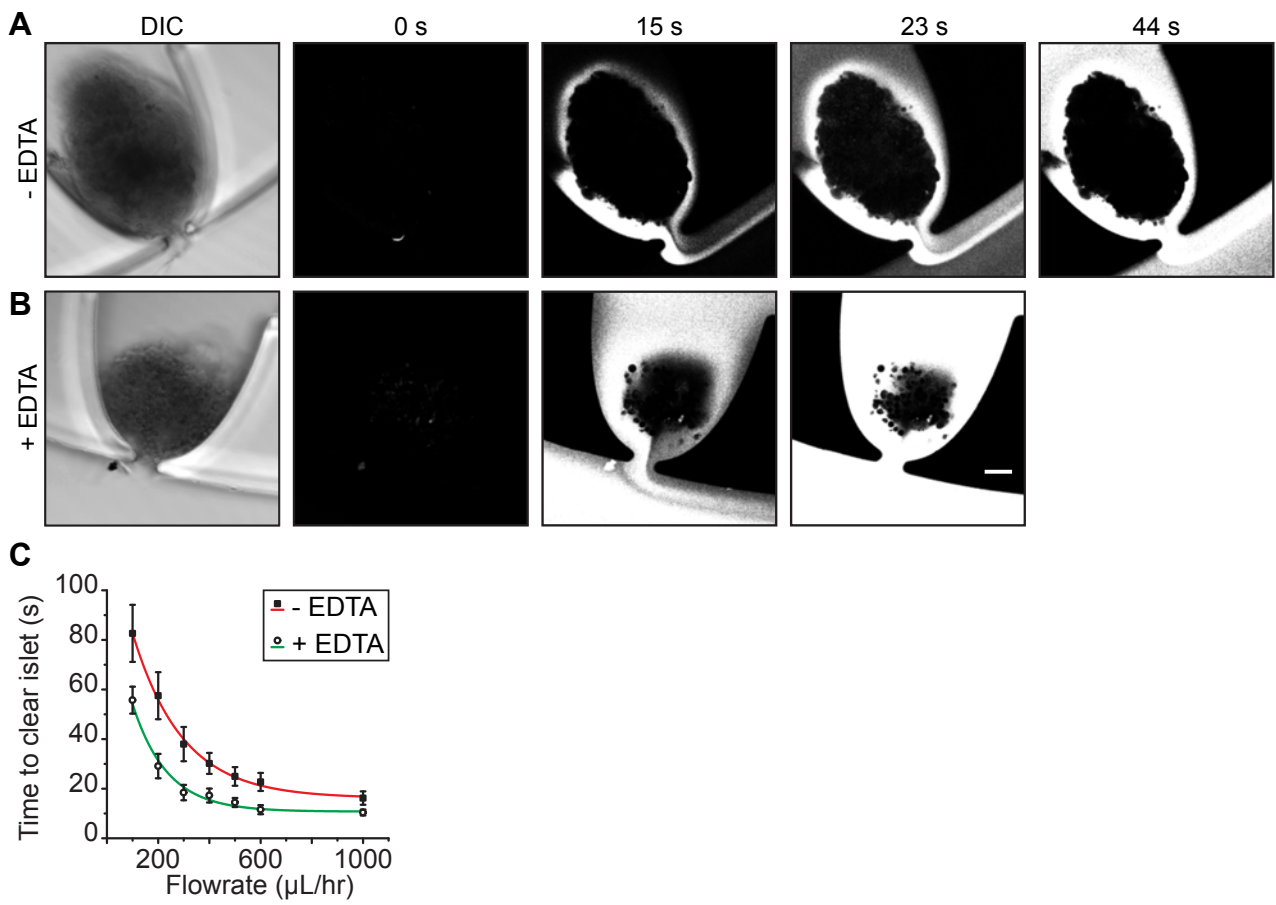


Figure S4

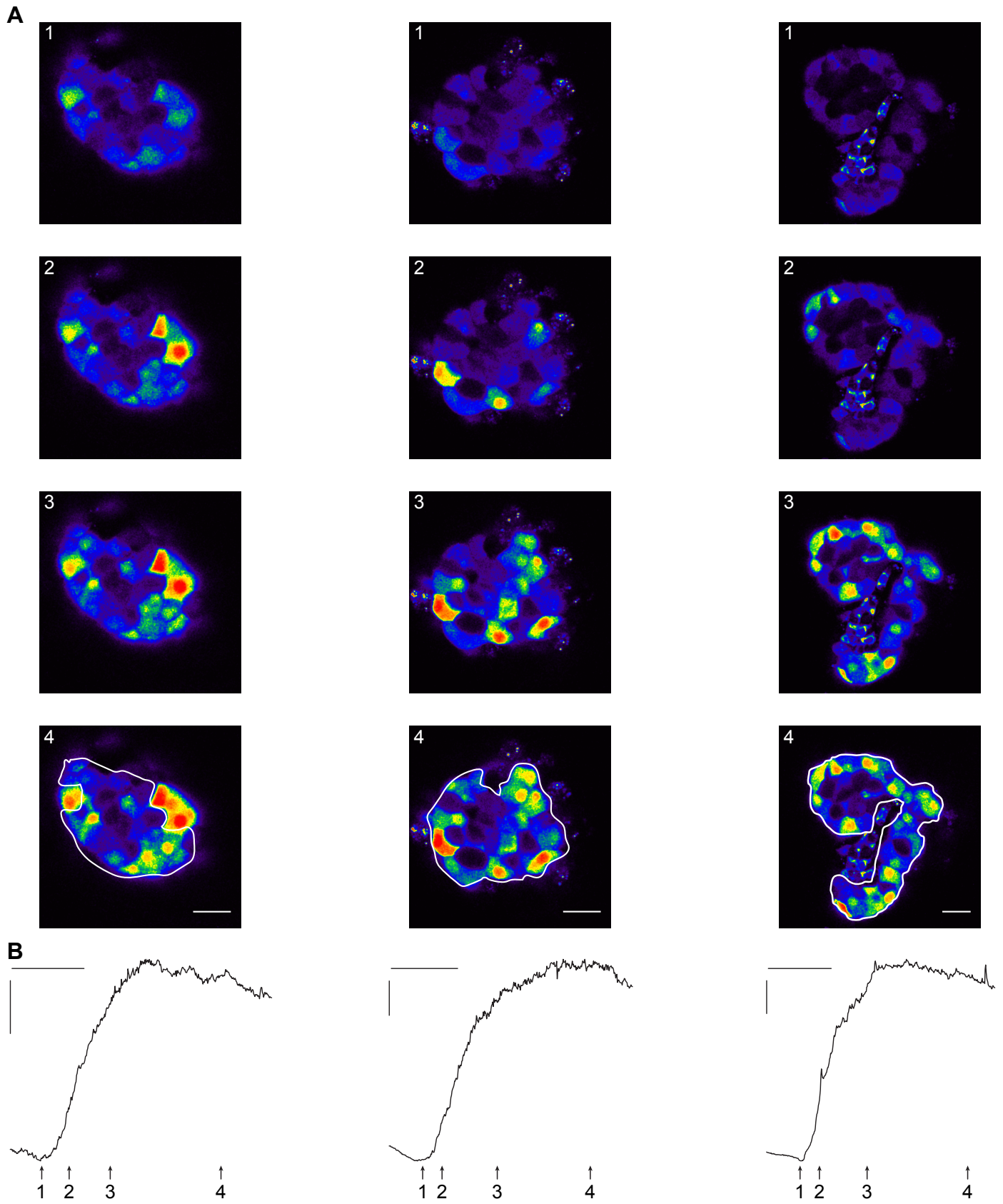


Figure S5